Biointerface Research in Applied Chemistry
Open-Access Journal (ISSN: 2069-5837)

Article
Volume 13, Issue 5, 2023, 460
https://doi.org/10.33263/BRIAC135.460

Covalent Inhibition for SARS-CoV-2 M pro via Zinc Ion Transported by Hydroxychloroquine: Investigated by DFT, ADMET and Molecular Docking

Rageh K. Hussein [1,*], Ahmed M. El-Khayatt [1], Ahmed M. Alkaoud [1], Ghada A. Khouqeer [1], Ahmed M. Deghady [2]

[1] Physics Department, College of Science, Imam Mohammad Ibn Saud Islamic University (IMSIU), Riyadh 11623, Saudi Arabia; rahussein@imamu.edu.sa (R.K.H); amelkhayatt@imamu.edu.sa (A.M.E); akaoud@imamu.edu.sa (A.M.A.); gkhouqeer@imamu.edu.sa (G.K.);
[2] Basic Science Department, Higher Technological Institute, 10th of Ramadan City 44629, Egypt; am_deghady@yahoo.com (A.M.D.);
* Correspondence: rahussein@imamu.edu.sa (R.K.H);

Scopus Author ID 57223388956
Received: 7.09.2022; Accepted: 9.10.2022; Published: 24.12.2022

Abstract: Improving the efficacy of hydroxychloroquine (HCQ) by several additives was one of the different strategies used to combat SARS-CoV-2. The most contentious issue in this regard was the transport of zinc ions by HCQ molecule. In this work, a design for HCQ binding to zinc ion (HCQZn) was screened to explore the role of zinc on the inhibitory activity of HCQ. Chemical descriptions and characterization of the designed molecule were obtained using DFT calculations. The detailed analysis of Drug-likeness and ADMET data yielded efficient pharmacological properties for HCQZn. Molecular docking investigation showed that HCQZn had a higher binding affinity (B.E. =-8.10 kcal/mol, Ki =1.15 µM) than HCQ, causing stronger binding within the cavity of SARS-CoV-2 main protease. Unexpectedly, zinc in the HCQ molecule formed three covalent bonds with the GLN189 amino acid residue. This is an extraordinary result because none of any conventional protocols for covalent molecular docking were used besides forming three covalent bonds by a single amino acid. This study identified HCQZn as an efficient covalent drug that could be a potential hit against SARS-CoV-2, and more clinical validation is essential to explore the potential risks of covalent drugs.

Keywords: Zinc Ion; Hydroxychloroquine; SARS-CoV-2; DFT; ADMET; Molecular Docking

1. Introduction

As the COVID-19 pandemic continues and new variants emerge, there is still an urgent need for a well-defined COVID-19 treatment or therapeutics. Hydroxychloroquine (HCQ) and several other drugs are being trialed to treat serious infections caused by this disease. Numerous works described these efforts that evaluated clinical trials of azithromycin, remdesivir, chloroquine, and natural products as symptomatic adjuvant therapy. [1-4]. Zinc is a valuable metal in medicinal chemistry, and it serves a variety of activities in the human body, including improving growth and catalytic functions. Since it has been discovered in hundreds of known enzymes called zinc metalloenzymes, zinc has been demonstrated to be essential for many enzymatic actions [5, 6]. Zn ion binding to catalytic or structural domains of various proteins is critical in defining their conformational changes, not only in humans but also in many viruses. Zinc ions or zinc complexes have received considerable attention as a potential

treatment for viral infections. The biological characteristics of zinc oxide have led to its widespread use in biomedical applications, particularly in anticancer and antibacterial treatment [7-9]. Growing respiratory viruses were treated with nanomaterial containing zinc [10]. Furthermore, various investigations have been conducted on using zinc alone or in combination with other drugs in the treatment of COVID-19. For example, Zn-ejector drugs were mixed with disulfiram and ebselen to inhibit mutational hotspots required for SARS-CoV-2 replication [11]. Chloroquine (CQ)/HCQ has been discussed frequently as a zinc ionophore, and the treatment of COVID-19 with zinc ions supplied by CQ/HCQ was found to be an effective strategy for minimizing morbidity and mortality [12-14]. The issue is that there is still no conception (to the best of our knowledge) about how zinc ions interact with CQ/HCQ molecules or for the configured structure of the Zn-CQ/HCQ combination. This was tackled as an objective to be demonstrated during this work.

Molecular docking simulations are becoming increasingly prominent in the scientific study due to their improved approaches and efficient methodologies in the field of drug discovery. Several previously published studies used molecular docking techniques to explore a wide spectrum of biological aspects in potential novel drugs, which aid in screening and selecting compounds so that they can be evaluated in clinical trials [15-18]. In the fight against COVID-19, computer-aided molecular docking modeling has proven to be exceptionally capable of recognizing and prescribing various treatment modalities [19-22].

The formation of one or more covalent chemical bonds between the inhibitor drug and the therapeutic target protein distinguishes covalent drugs from non-covalent ones. Many well-known drugs are now described using the covalent mechanism, such as Clopidogrel, Telaprevir, Afatinib, and others. Covalent medicines have long been considered a risk issue in pharmaceutical research due to the possibility of causing acute cellular damage, toxic effects, or inducing an immune response, even though they have proven to be effective therapies for a variety of medical conditions owing to increased drug efficiency and longer duration of the activity, as well as the ability to target deep binding sites [23- 25]. Discovering or designing safe covalent drugs that do not cause toxicity, drug resistance, or mutations is currently a major challenge [26, 27]. Regarding molecular covalent docking as a sophisticated process with protocols and certain criteria, the formation of a covalent bond is still a complicated task to describe accurately.

The scope of this study is to expand the level of knowledge on the mechanism of HCQ as a zinc ionophore by applying Density Functional Theory (DFT) calculations to optimize a molecular structure that illustrates how the zinc ion binds with HCQ. The proposed HCQZn ligand was then compared to HCQ in an in silico study to assess its effectiveness against COVID-19. To this end, a set of Drug-likeness and ADMET (absorption, distribution, metabolism, excretion, and toxicity) calculations were employed to identify the bioavailability, pharmacokinetic characteristics, and safety validation in the context of potential drug candidates. Then, a molecular docking technique identified the efficacy of inhibiting the main protease (M pro) of SARS-CoV-2.

2. Materials and Methods

2.1. Chemistry and DFT calculations.

HCQ could be a zinc transporter due to its high propensity for forming stable complexes with zinc ions via coordination bonds. This is done by sharing the lone pair electrons of the

hydroxyl and amine groups in HCQ with the zinc ion. The designed HCQZn ligand was subjected to density functional theory (DFT) calculations and HCQ to determine the geometrical structure and some of their chemical parameters. In DFT, geometry optimization calculation was used to locate the ground state using the Becke3-Lee-Yang-Parr (B3LYP) exchange-correlation functional and the 6-311** basis set [28, 29]. DFT computations were carried out with the Gaussian 09 package program [30].

2.2. Drug likeness and ADMET profile.

The pkCSM web server was used to predict drug-likeness, and ADMET features in order to describe the biopharmaceutical aspects of the ligands under study [31]. The Molinspiration program was also used to validate further the calculated Lipinski rules (Molinspiration Cheminformatics free web services, https://www.molinspiration.com)

2.3. Molecular docking.

The SARS-CoV-2 M pro crystal structure (PDB ID: 6LU7) was obtained from the Protein Data Bank site. Auto dock Tools 1.5.6 software was used for molecular docking calculations [32]. Several steps were taken to prepare 6LU7 protein, including removing water molecules, assigning gasteiger partial charges, and adding polar hydrogen. The optimized HCQZn ligand from DFT calculations was inserted into AutoDockTools and combined with the 6LU7 protein. The ligand's torsion tree was set up by detecting the roots, then PDBQT files were created for both the ligand and the M pro protease. The M pro was centered within a grid box with dimensions of 40 × 40 ×40 points in x, y, z directions and grid spacing of 0.375 Å. Finally, the Lamarckian genetic algorithm (LGA) was used to perform the molecular docking procedure. The ligand binding interaction within the cavity Mpro protein was visualized using Discovery Studio 4.5 [33]

3. Results and Discussion

3.1. DFT calculations.

Figure 1 illustrates the molecular structures of HCQ and HCQZn, as well as their optimized structures. The optimized structure of HCQZn reveals that the Zn ion is located behind the hydroxyl and amine groups, and the HCQ chain structure was modified to a nearly circular configuration due to the interaction between the Zn ion and N, O atoms. This modification profits HCQZn's good oral bioavailability by reducing the polar surface area, as discussed in section 3.1.

Table 1 shows how to employ model chemistry, such as Koopmans' theorem [34], to calculate some chemical reactivity descriptors for the studied compounds based on the electronic properties determined. Chemical descriptors, including the energy gap ΔE, chemical hardness η and softness σ, which are derived from ionization potential (I) and electron affinity (A), are significant tools for identifying the chemical reactivity or stability of compounds. A high ΔE value refers to high chemical stability, whereas a small ΔE value is correlated with high reactivity. The activity of a molecule in a chemical reaction is determined by its hardness or softness. In chemical reactions, a hard molecule with a high η value resists changes in its electronic distribution, while a soft molecule with a high σ value reacts faster than a hard molecule. Based on the obtained chemical parameters in Table 1, HCQZn has a smaller energy

gap, lower hardness value, and higher softness value than HCQ. These results indicate that HCQZn has a higher chemical reactivity than HCQ.

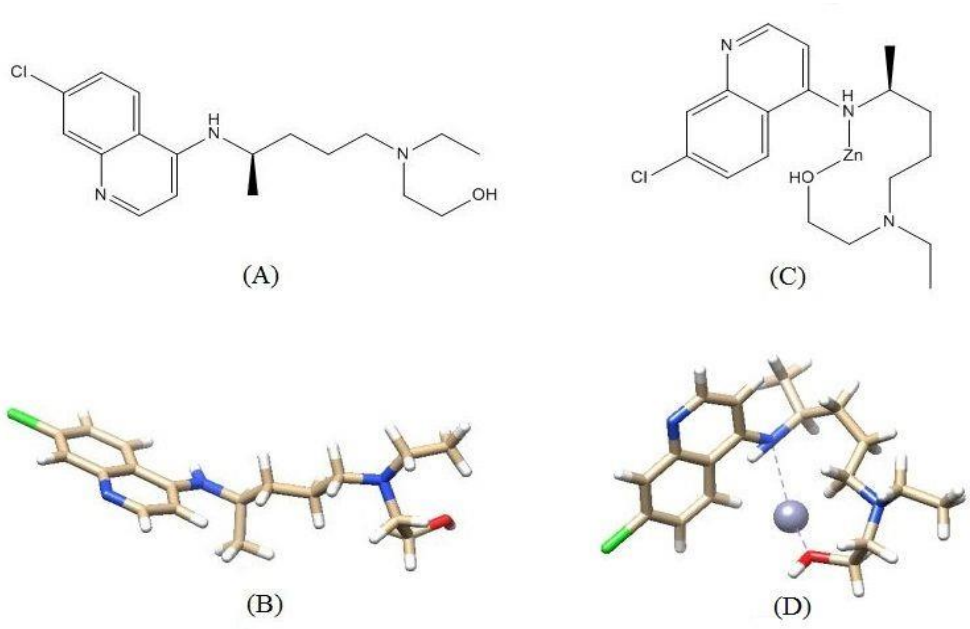

Figure 1. Molecular and optimized structures of HCQ **(A)** and **(B),** and also HCQZn **(C)** and **(D).**

Table 1. Chemical reactivity descriptors for HCQ and HCQZn.

	E_{HOMO} (eV)	E_{LUMO} (eV)	ΔE (eV)	I (eV)	A (eV)	η (eV)	σ $(eV)^{-1}$	χ	ω
Defination	——	——	$\Delta E = E_{LUMO} - E_{HOMO}$	$-E_{HOMO}$	$-E_{LUMO}$	$\frac{I-A}{2}$	$\frac{1}{\eta} = \frac{1}{I-A}$	$\frac{-(E_H + E_L)}{2}$	$\frac{\chi^2}{2\eta}$
HCQ	-5.96	-1.59	4.37	5.96	1.59	2.185	0.46	3.78	4.31
HCQZn	-4.49	-1.01	3.48	4.49	1.01	1.74	0.57	2.75	2.17

3.2. Drug likeness and ADMET evaluation.

Drug development necessitates the use of appropriate physicochemical and biopharmaceutical parameters. Drug-likeness is a criterion for the standard properties required for the selection of potential drug compounds. Lipinski's "rule of five," can be used to achieve drug-likeness. The rule specifies the following components; molecular weight (MW), hydrogen bond donors (HBD), hydrogen bond acceptors (HBA), and octanol/water partition coefficient (log P) [35]. Another set of rules relating the polar surface area (PSA) and the number of rotatable bonds (ROTB) to good oral bioavailability drugs. Previously, a database of oral bioavailability for over 1000 compounds was investigated, and it was concluded that drugs with PSA <140 Å² and ROTB <10 had the properties of successful oral bioavailability drugs [36].

The drug-likeness and associated properties, such as PSA and ROTB, are shown in Table 2. The HCQZn satisfies the criteria of drug-likeness based on the rule of five with zero violations. Lipophilicity, which results in high LogP values, indicates poor permeation and increase hazard attrition. Paul Leeson and Brian Springthorpe confirmed that a low level of LogP is a key to successful drug discovery [37]. As shown in Table 2, Zn increased the lipophilicity of HCQ by lowering the LogP value. TPSA for HCQZn was significantly lower than for HCQ. The reduction of the TPSA is a noticeable indicator of good oral bioavailability [38].

Table 2. Predicted drug-likeness parameters for HCQ and HCQZn.

Parameter	MW (g/mol)	LogP	HBD	HBA	PSA (Å²)	ROTB
rule of five	< 500	≤ 5	≤ 5	≤ 10	<140	≤ 10
HCQ	355.88	3.78	2	4	48.38	9
HCQZn	401.27	2.35	2	4	34.90	2

Absorption, distribution, metabolism, and excretion are the four components (ADME) of new drug candidates' pharmacokinetic properties. After the toxicological evaluation was included, the ADMET profile was recently addressed. The ADMET study is an excellent starting point for understanding the pharmacokinetic aspects associated with drug design. Good drug candidates must have favorable ADME characteristics as well as be non-toxic [39]. Therefore, predicting ADMET properties is considered a significant step in indicating the successful pathway of a drug in clinical treatments.

The results of Table 3 show the various ADMET properties that were obtained, and the most important aspects of these outcomes will be discussed. The solubility parameter (log S) is an important factor in determining the efficacy of drug bioavailability; high log S values are associated with good drug absorption. The following are the water solubility criteria: strong soluble 0 > soluble >-4 > moderate>-6 > poorly > -10 > insoluble [40]. The solubility of HCQZn was improved as the log S value increased from -3.323 to -2.636. The high solubility of HCQZn was evidenced by enhancing the human intestinal absorbance value to ≈ 94%. HCQZn has no inhibitory activity against P-glycoprotein I/II, which is important in drug formulations. HCQZn, with the same high value of VDss (the steady-state volume of distribution demonstrates the amount of drug required for uniformly distributed in blood and plasma) as HCQ , represents a drug with great distribution in plasma (VDss > 0.45) [42]. The ability of a drug to pass the blood-brain barrier (BBB) and thus impose its impact on the brain is an essential attribute of medicinal chemistry. BBB value <-1 for a given molecule indicates that it is poorly distributed to the brain [36]. The BBB permeability results show that HCQZn, like HCQ, is penetrating for BBB.

Table 3. The ADMET description for HCQ and HCQZn.

Property	Parameter/Model Name	Unit	HCQ	HCQZn
Absorption	Water solubility	Numeric (log mol/L)	− 3.323	− 2.636
	Skin permeability	Numeric (log kp)	− 2.971	−2.849
	Human Intestinal absorption	Numeric (% Absorbed)	88.445	93.849
	CaCo2 permeability	(log Papp in 10-6 cm/s)	1.47	1.061
	P-glycoprotein substrate	Categorical (Yes/No)	Yes	Yes
	P-glycoprotein I inhibitor	Categorical (Yes/No)	No	No
	P-glycoprotein II inhibitor	Categorical (Yes/No)	No	No
Distribution	VDss (human)	Numeric (log L/kg)	1.283	1.281
	BBB permeability	Numeric (log BB)	0.122	0.468
	Fraction unbounded	(Fu)	0.303	0.682
	CNS permeability	(log PS)	− 2.736	−3.058
Metabolism	CYP2D6 substrate	Categorical (Yes/No)	Yes	No
	CYP3A4 substrate	Categorical (Yes/No)	Yes	Yes
	CYP1A2 inhibitor	Categorical (Yes/No)	No	No
	CYP2C19 inhibitor	Categorical (Yes/No)	No	No
	CYP2C9 inhibitor	Categorical (Yes/No)	No	No
	CYP2D6 inhibitor	Categorical (Yes/No)	No	No
	CYP3A4 inhibitor	Categorical (Yes/No)	No	No
Excretion	Total Clearance	Numeric (log ml/min/kg)	1.132	1.598
	Renal OCT2 substrate	Categorical (Yes/No)	No	No
Toxicity	AMES toxicity	Categorical (Yes/No)	Yes	No
	Max. tolerated dose (human)	Numeric (log mg/kg/day)	0.191	−0.457
	hERG I inhibitor	Categorical (Yes/No)	No	No
	hERG II inhibitor	Categorical (Yes/No)	Yes	Yes
	Skin Sensitisation	Categorical (Yes/No)	No	No

Inhibiting cytochrome P450 enzymes may result in interactions between drugs, where co-administered drugs are not metabolized and build up to be toxic. None of these enzymes were inhibited by HCQZn, which is considered a safe agent when used in conjunction with other drugs. The constant of proportionality CLtot is an abbreviation for the total clearance of the drug (drug removal from blood or plasma) in terms of hepatic clearance and renal clearance; a high CLtot value indicates a faster drug excretion process [43]. According to the total clearance values predicted in Table 3, HCQZn has a higher CLtot value than HCQ, implying a faster excretion rate. HCQZn, unlike HCQ, is not mutagenic and has no AMES toxicity. The maximum tolerated dose (MRDT) of a chemical in humans is a measurement of its hazardous dosage threshold. A low MRTD value is defined as ≤ 0.477 log (mg/kg/day), whereas toxic chemicals have an MRTD vastly larger than 0.477 log (mg/kg/day) [44]. HCQZn has a lower MRTD limit that is safer than HCQ.

2.3. Molecular docking.

The binding energy (B.E.) and inhibition constant (Ki) are both measures of a drug's affinity for its target protein, a high level of binding affinity is indicated by lower values of the B. E. and Ki values [45]. Table 4 provides the docking results of HCQ and HCQZn with the target protein. Molecular docking of HCQ with 6lu7 M pro was reported in several studies with widely accepted results; the findings of the current study, which have a binding energy of-6.87 kcal/Mol and inhibition constant of 9.15 µM are consistent with previous studies [46, 47]. The docking score of HCQ Zn reveals a stronger affinity and more stable complex of HCQ Zn-M pro indicated by a lower stable energy of -8.10 kcal/mol, and a smaller value of K_i 1.15 µM.

Table 4. The calculated binding energies and inhibition constant (Ki) of docked HCQ and HCQZn ligands within the M pro of SARS-CoV-2.

No,	Protein	Compound	Binding energy B. E. (kcal/mol)	Inhibition Constant K_i (µM)	Ligand efficiency
1	6lu7	HCQ	- 6.87	9.15	-0.30
2		HCQZn	-8.10	1.15	-0.34

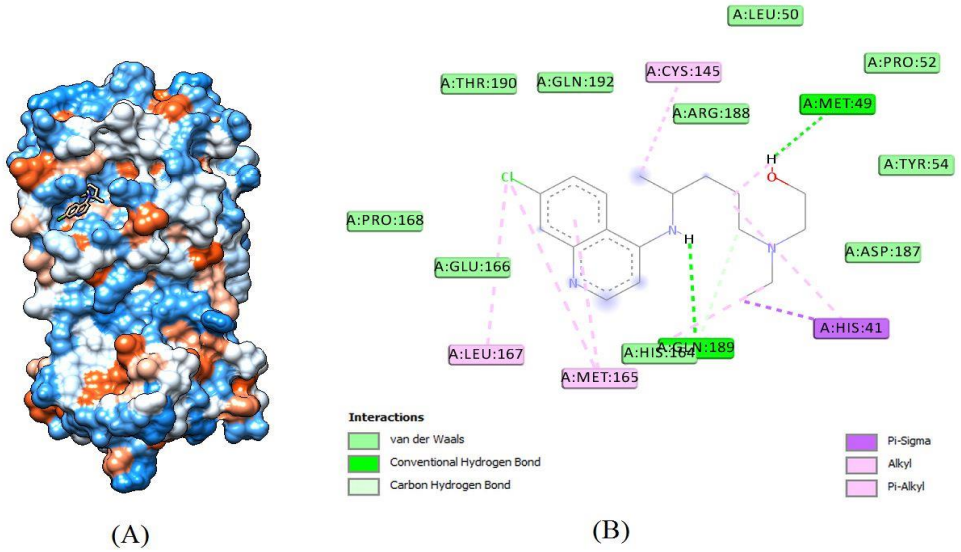

Figure 2. (A) 3D solid surface representation of HCQ-6lu7 complex. **(B)** 2D surface representation for the interactions of HCQ within the active site of 6lu7 receptor.

The ligand-binding site interactions in the active site of the 6lu7 M pros were depicted in Figure 2 and Figure 3. In line with many earlier studies, the interactions of HCQ with amino

acid residues of the 6lu7 receptor cavity are mainly classical and hydrophobic, with two hydrogen bonds formed [47]. However, the docked pose of the HCQZn-M pro complex yielded an interesting result, where the zinc ion added to HCQ was able to form three covalent bonds with the GLN189 residue (Figure 3B). This docking's findings highlight two important points. First, the normal molecular docking procedure was employed (as indicated in the material and methods section) without any covalent molecular docking protocols. Second, the fact that all three covalent bonds were formed with the same GLN189 residue is a question mark; since highly selective covalent drugs can target rare residues of a specific targeted protein [48], this result will draw more attention to the GLN189 residue. Finally, the formed covalent bonds revealed higher binding affinity HCQZn, suggesting that it is a strong candidate for SARS-CoV-2 treatment.

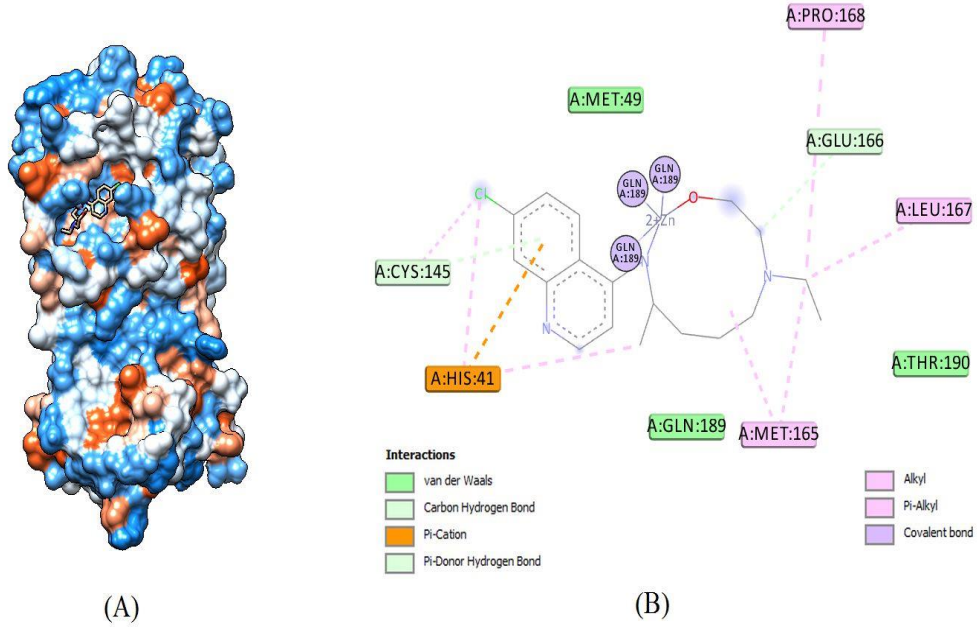

Figure 3. (A) 3D solid surface representation of HCQZn-6lu7 complex. **(B)** 2D surface representation 197 for the interactions of HCQZn within the active site of 6lu7 receptor.

4. Conclusions

In the ongoing search for an effective SARS-CoV-2 treatment drug, this study focused on the impact of zinc ions transported by HCQ molecule as a potential inhibitor of the SARS-CoV-2 target protein. A series of molecular modeling investigations were performed on a designed HCQ-Zn ligand. In evaluating Drug-likeness and ADMET, the proposed ligand revealed various positive pharmacokinetic properties. Then, molecular docking of the HCQZn ligand was performed within the cavity of the main protease of SARS-CoV-2. The HCQ Zn-M pro complex's docked pose exhibited impressive covalent interaction; three covalent bonds were formed between zinc in the HCQ complex and the GLN 189 amino acid. This result revealed HCQZn to be a potent covalent drug with a considerably higher binding affinity for M pro than the conventional non-covalent interaction in HCQ.

Funding

This research was supported by the Deanship of Scientific Research, Imam Mohammad Ibn Saud Islamic University (IMSIU), Saudi Arabia, Grant No. (21-13-18-061).

Acknowledgments

This research was supported by the Deanship of Scientific Research, Imam Mohammad Ibn Saud Islamic University (IMSIU), Saudi Arabia, Grant No. (21-13-18-061).

Conflicts of Interest

The authors declare no conflict of interest.

References

1. Gautret, P.; Lagier, J.-C.; Parola, P.; Hoang, V. T.; Meddeb, L.; Mailhe, M.; Doudier, B.; Courjon, J.; Giordanengo, V.; Vieira, V. E.; Tissot Dupont, H.; Honoré, S.; Colson, P.; Chabrière, E.; La Scola, B.; Rolain, J.-M.; Brouqui, P.; Raoult, D. Hydroxychloroquine and Azithromycin as a Treatment of COVID-19: Results of an Open-Label Non-Randomized Clinical Trial. *International Journal of Antimicrobial Agents* **2020**, *56* , 105949, https://doi.org/10.1016/j.ijantimicag.2020.105949.
2. Beigel, J. H.; Tomashek, K. M.; Dodd, L. E.; Mehta, A. K.; Zingman, B. S.; Kalil, A. C.; Hohmann, E.; Chu, H. Y.; Luetkemeyer, A.; Kline, S.; Lopez de Castilla, D.; Finberg, R. W.; Dierberg, K.; Tapson, V.; Hsieh, L.; Patterson, T. F.; Paredes, R.; Sweeney, D. A.; Short, W. R.; Touloumi, G.; Lye, D. C.; Ohmagari, N.; Oh, M.; Ruiz-Palacios, G. M.; Benfield, T.; Fätkenheuer, G.; Kortepeter, M. G.; Atmar, R. L.; Creech, C. B.; Lundgren, J.; Babiker, A. G.; Pett, S.; Neaton, J. D.; Burgess, T. H.; Bonnett, T.; Green, M.; Makowski, M.; Osinusi, A.; Nayak, S.; Lane, H. C. Remdesivir for the Treatment of Covid-19 — Final Report. *N Engl J Med* **2020**, *383*, 1813–1826, https://doi.org/10.1056/NEJMoa2007764.
3. Rana, D. R.; Dulal, S. A Review of Dosages of Chloroquine and Hydroxychloroquine for COVID-19 in Registered Clinical Trials during First Quarter of 2020; preprint. *Pharmacology and Therapeutics* **2020**, https://doi.org/10.1101/2020.03.22.20040964.
4. Silveira, D.; Prieto-Garcia, J. M.; Boylan, F.; Estrada, O.; Fonseca-Bazzo, Y. M.; Jamal, C. M.; Magalhães, P. O.; Pereira, E. O.; Tomczyk, M.; Heinrich, M. COVID-19: Is There Evidence for the Use of Herbal Medicines as Adjuvant Symptomatic Therapy? *Front. Pharmacol.* **2020**, *11*, 581840, https://doi.org/10.3389/fphar.2020.581840.
5. McCall, K. A.; Huang, C.; Fierke, C. A. Function and Mechanism of Zinc Metalloenzymes. *The Journal of Nutrition* **2000**, *130*, 1437S-1446S. https://doi.org/10.1093/jn/130.5.1437S.
6. Maret, W. Zinc Biochemistry: From a Single Zinc Enzyme to a Key Element of Life. *Advances in Nutrition* **2013**, *4* , 82–91, https://doi.org/10.3945/an.112.003038 .
7. Lallo da Silva, B.; Abuçafy, M. P.; Berbel Manaia, E.; Oshiro Junior, J. A.; Chiari-Andréo, B. G.; Pietro, R. C. R.; Chiavacci, L. A. Relationship Between Structure And Antimicrobial Activity Of Zinc Oxide Nanoparticles: An Overview. *IJN* **2019**, *14*, 9395–9410, https://doi.org/10.2147/IJN.S216204.
8. Jiang, J.; Pi, J.; Cai, J. The Advancing of Zinc Oxide Nanoparticles for Biomedical Applications. *Bioinorganic Chemistry and Applications* **2018**, *2018*, 1–18. https://doi.org/10.1155/2018/1062562.
9. Ngoepe, M. P.; Clayton, H. S. Metal Complexes as DNA Synthesis and/or Repair Inhibitors: Anticancer and Antimicrobial Agents. *Pharmaceutical Fronts* **2021**, *03* , e164–e182, https://doi.org/10.1055/s-0041-1741035.
10. Gutiérrez Rodelo, C.; Salinas, R. A.; Armenta Jaime, E.; Armenta, S.; Galdámez-Martínez, A.; Castillo-Blum, S. E.; Astudillo-de la Vega, H.; Nirmala Grace, A.; Aguilar-Salinas, C. A.; Gutiérrez Rodelo, J.; Christie, G.; Alsanie, W. F.; Santana, G.; Thakur, V. K.; Dutt, A. Zinc Associated Nanomaterials and Their Intervention in Emerging Respiratory Viruses: Journey to the Field of Biomedicine and Biomaterials. *Coordination Chemistry Reviews* **2022**, *457*, 214402, https://doi.org/10.1016/j.ccr.2021.214402.
11. Sargsyan, K.; Lin, C.-C.; Chen, T.; Grauffel, C.; Chen, Y.-P.; Yang, W.-Z.; Yuan, H. S.; Lim, C. Multi-Targeting of Functional Cysteines in Multiple Conserved SARS-CoV-2 Domains by Clinically Safe Zn-Ejectors. *Chem. Sci.* **2020**, *11*, 9904–9909, https://doi.org/10.1039/D0SC02646H.
12. Xue, J.; Moyer, A.; Peng, B.; Wu, J.; Hannafon, B. N.; Ding, W.-Q. Chloroquine Is a Zinc Ionophore. *PLoS ONE* **2014**, *9*, e109180, https://doi.org/10.1371/journal.pone.0109180.
13. Derwand, R.; Scholz, M. Does Zinc Supplementation Enhance the Clinical Efficacy of Chloroquine/Hydroxychloroquine to Win Today's Battle against COVID-19? *Medical Hypotheses* **2020**, *142*, 109815, https://doi.org/10.1016/j.mehy.2020.109815.

14. Abd-Elsalam, S.; Soliman, S.; Esmail, E. S.; Khalaf, M.; Mostafa, E. F.; Medhat, M. A.; Ahmed, O. A.; El Ghafar, M. S. A.; Alboraie, M.; Hassany, S. M. Do Zinc Supplements Enhance the Clinical Efficacy of Hydroxychloroquine?: A Randomized, Multicenter Trial. *Biol Trace Elem Res* **2021**, *199*, 3642–3646, https://doi.org/10.1007/s12011-020-02512-1.
15. Joshi, B. P.; Bhandare, V. V.; Patel, P.; Sharma, A.; Patel, R.; Krishnamurthy, R. Molecular Modelling Studies and Identification of Novel Phytochemical Inhibitor of DLL3. *Journal of Biomolecular Structure and Dynamics* **2022**, 1–21, https://doi.org/10.1080/07391102.2022.2045224.
16. Gurung, A. B.; Ali, M. A.; Lee, J.; Farah, M. A.; Al-Anazi, K. M. Molecular Docking and Dynamics Simulation Study of Bioactive Compounds from Ficus Carica L. with Important Anticancer Drug Targets. *PLoS ONE* **2021**, *16*, e0254035, https://doi.org/10.1371/journal.pone.0254035.
17. Noor, F.; Rehman, A.; Ashfaq, U. A.; Saleem, M. H.; Okla, M. K.; Al-Hashimi, A.; AbdElgawad, H.; Aslam, S. Integrating Network Pharmacology and Molecular Docking Approaches to Decipher the Multi-Target Pharmacological Mechanism of Abrus Precatorius L. Acting on Diabetes. *Pharmaceuticals* **2022**, *15*, 414, https://doi.org/10.3390/ph15040414 .
18. Saddique, F. A.; Ahmad, M.; Ashfaq, U. A.; Muddassar, M.; Sultan, S.; Zaki, M. E. A. Identification of Cyclic Sulfonamides with an N-Arylacetamide Group as α-Glucosidase and α-Amylase Inhibitors: Biological Evaluation and Molecular Modeling. *Pharmaceuticals* **2022**, *15*, 106, https://doi.org/10.3390/ph15010106.
19. Vijayakumar, M.; Janani, B.; Kannappan, P.; Renganathan, S.; Al-Ghamdi, S.; Alsaidan, M.; Abdelaziz, M. A.; Peer Mohideen, A.; Shahid, M.; Ramesh, T. In Silico Identification of Potential Inhibitors against Main Protease of SARS-CoV-2 6LU7 from Andrographis Panniculata via Molecular Docking, Binding Energy Calculations and Molecular Dynamics Simulation Studies. *Saudi Journal of Biological Sciences* **2022**, *29*, 18–29, https://doi.org/10.1016/j.sjbs.2021.10.060.
20. Rutwick Surya, U.; Praveen, N. A Molecular Docking Study of SARS-CoV-2 Main Protease against Phytochemicals of Boerhavia Diffusa Linn. for Novel COVID-19 Drug Discovery. *VirusDis.* **2021**, *32*, 46–54, https://doi.org/10.1007/s13337-021-00683-6.
21. Hosseini, M.; Chen, W.; Xiao, D.; Wang, C. Computational Molecular Docking and Virtual Screening Revealed Promising SARS-CoV-2 Drugs. *Precision Clinical Medicine* **2021**, *4*, 1–16, https://doi.org/10.1093/pcmedi/pbab001.
22. Islam, R.; Parves, Md. R.; Paul, A. S.; Uddin, N.; Rahman, Md. S.; Mamun, A. A.; Hossain, Md. N.; Ali, Md. A.; Halim, M. A. A Molecular Modeling Approach to Identify Effective Antiviral Phytochemicals against the Main Protease of SARS-CoV-2. *Journal of Biomolecular Structure and Dynamics* **2020**, 1–12, https://doi.org/10.1080/07391102.2020.1761883.
23. Singh, J.; Petter, R. C.; Baillie, T. A.; Whitty, A. The Resurgence of Covalent Drugs. *Nat Rev Drug Discov* **2011**, *10*, 307–317, https://doi.org/10.1038/nrd3410.
24. Sutanto, F.; Konstantinidou, M.; Dömling, A. Covalent Inhibitors: A Rational Approach to Drug Discovery. *RSC Med. Chem.* **2020**, *11*, 876–884, https://doi.org/10.1039/D0MD00154F.
25. Bauer, R. A. Covalent Inhibitors in Drug Discovery: From Accidental Discoveries to Avoided Liabilities and Designed Therapies. *Drug Discovery Today* **2015**, *20*, 1061–1073, https://doi.org/10.1016/j.drudis.2015.05.005.
26. Cheng, S.-S.; Yang, G.-J.; Wang, W.; Leung, C.-H.; Ma, D.-L. The Design and Development of Covalent Protein-Protein Interaction Inhibitors for Cancer Treatment. *J Hematol Oncol* **2020**, *13*, 26. https://doi.org/10.1186/s13045-020-00850-0.
27. Vale, N. *Biomedical Chemistry: Current Trends and Developments*; De Gruyter Open Poland, 2015, https://doi.org/10.1515/9783110468755.
28. Hertwig, R. H.; Koch, W. On the Parameterization of the Local Correlation Functional. What Is Becke-3-LYP? *Chemical Physics Letters* **1997**, *268* , 345–351. https://doi.org/10.1016/S0009-2614(97)00207-8.
29. Raghavachari, K. Perspective on "Density Functional Thermochemistry. III. The Role of Exact Exchange." *Theoretical Chemistry Accounts: Theory, Computation, and Modeling (Theoretica Chimica Acta)* **2000**, *103*, 361–363, https://doi.org/10.1007/s002149900065.
30. Frisch, M.J.; Trucks, G.W.; Schlegel, H.B. Gaussian 09; Gaussian Inc.: Wallingford, CT, USA, **2009**, https://www.cwu.edu/chemistry/sites/cts.cwu.edu.chemistry/files/documents/Gaussian_09_ReferenceManual.pdf.
31. Pires, D. E. V.; Blundell, T. L.; Ascher, D. B. PkCSM: Predicting Small-Molecule Pharmacokinetic and Toxicity Properties Using Graph-Based Signatures. *J. Med. Chem.* **2015**, *58*, 4066–4072, https://doi.org/10.1021/acs.jmedchem.5b00104.

32. Morris, G. M.; Huey, R.; Lindstrom, W.; Sanner, M. F.; Belew, R. K.; Goodsell, D. S.; Olson, A. J. AutoDock4 and AutoDockTools4: Automated Docking with Selective Receptor Flexibility. *J. Comput. Chem.* **2009**, *30*, 2785–2791, https://doi.org/10.1002/jcc.21256.
33. Dassault Systèmes BIOVIA. Discovery Studio Modelling Environment, Release 2017; Dassault Systèmes: San Diego, CA, USA, 2016.
34. Tsuneda, T.; Song, J.-W.; Suzuki, S.; Hirao, K. On Koopmans' Theorem in Density Functional Theory. *The Journal of Chemical Physics* **2010**, *133*, 174101, https://doi.org/10.1063/1.3491272.
35. Lipinski, C. A. Lead- and Drug-like Compounds: The Rule-of-Five Revolution. *Drug Discovery Today: Technologies* **2004**, *1*, 337–341, https://doi.org/10.1016/j.ddtec.2004.11.007.
36. Veber, D. F.; Johnson, S. R.; Cheng, H.-Y.; Smith, B. R.; Ward, K. W.; Kopple, K. D. Molecular Properties That Influence the Oral Bioavailability of Drug Candidates. *J. Med. Chem.* **2002**, *45* , 2615–2623, https://doi.org/10.1021/jm020017n.
37. Leeson, P. D.; Springthorpe, B. The Influence of Drug-like Concepts on Decision-Making in Medicinal Chemistry. *Nat Rev Drug Discov* **2007**, *6*, 881–890, https://doi.org/10.1038/nrd2445.
38. Egieyeh, S. A.; Syce, J.; Malan, S. F.; Christoffels, A. Prioritization of Anti-Malarial Hits from Nature: Chemo-Informatic Profiling of Natural Products with in Vitro Antiplasmodial Activities and Currently Registered Anti-Malarial Drugs. *Malar J* **2016**, *15*, 50, https://doi.org/10.1186/s12936-016-1087-y.
39. Hefti, F. F. Requirements for a Lead Compound to Become a Clinical Candidate. *BMC Neurosci* **2008**, *9*, (S3), S7, https://doi.org/10.1186/1471-2202-9-S3-S7.
40. Avdeef, A. Prediction of Aqueous Intrinsic Solubility of Druglike Molecules Using Random Forest Regression Trained with Wiki-PS0 Database. **2020**, *49*, https://doi.org/10.5599/admet.766.
41. Saha, S.; Nandi, R.; Vishwakarma, P.; Prakash, A.; Kumar, D. Discovering Potential RNA Dependent RNA Polymerase Inhibitors as Prospective Drugs Against COVID-19: An in Silico Approach. *Front. Pharmacol.* **2021**, *12*, 634047, https://doi.org/10.3389/fphar.2021.634047.
42. Vilar, S.; Chakrabarti, M.; Costanzi, S. Prediction of Passive Blood–Brain Partitioning: Straightforward and Effective Classification Models Based on in Silico Derived Physicochemical Descriptors. *Journal of Molecular Graphics and Modelling* **2010**, *28*, 899–903, https://doi.org/10.1016/j.jmgm.2010.03.010.
43. Hardjono, S.; Siswandono, S.; Andayani, R. Evaluation of N-Benzoylthiourea Derivatives as Popssible Analgesic Agents by Predicting Their Hysicochemical and Pharmacokinetic Properties, Toxicity, and Analgesic Activity. *Indones. J. Biotechnol.* **2018**, *22*, 76, https://doi.org/10.22146/ijbiotech.27171.
44. Pires, D. E. V.; Blundell, T. L.; Ascher, D. B. PkCSM: Predicting Small-Molecule Pharmacokinetic and Toxicity Properties Using Graph-Based Signatures. *J. Med. Chem.* **2015**, *58*, 4066–4072, https://doi.org/10.1021/acs.jmedchem.5b00104.
45. Thafar, M.; Raies, A. B.; Albaradei, S.; Essack, M.; Bajic, V. B. Comparison Study of Computational Prediction Tools for Drug-Target Binding Affinities. *Front. Chem.* **2019**, *7*, 782, https://doi.org/10.3389/fchem.2019.00782.
46. Cheke, R. S. The Molecular Docking Study of Potential Drug Candidates Showing Anti-COVID-19 Activity by Exploring of Therapeutic Targets of SARS-CoV-2. *EJMO* **2020**, https://doi.org/10.14744/ejmo.2020.31503.
47. Hussein, R. K.; Elkhair, H. M. Molecular Docking Identification for the Efficacy of Some Zinc Complexes with Chloroquine and Hydroxychloroquine against Main Protease of COVID-19. *Journal of Molecular Structure* **2021**, *1231*, 129979, https://doi.org/10.1016/j.molstruc.2021.129979.
48. Kumalo, H.; Bhakat, S.; Soliman, M. Theory and Applications of Covalent Docking in Drug Discovery: Merits and Pitfalls. *Molecules* **2015**, *20*, 1984–2000, https://doi.org/10.3390/molecules20021984.